Available online at www.sciencedirect.com
ScienceDirect
Electric Power Systems Research 77 (2007) 1028–1037
ELECTRIC POWER SYSTEMS RESEARCH
www.elsevier.com/locate/epsr

A linear approach to study the influence of asynchronous wind parks on isolated networks

C. Carrillo [a], A.E. Feijóo [a,*], J. Cidrás [a], J.F. Medina [b]

[a] Departamento de Enxeñería Eléctrica-Universidade de Vigo, ETSEI, Campus de Lagoas-Marcosende, Vigo, Spain
[b] Departamento de Ingeniería Eléctrica-Universidad de Las Palmas de Gran Canaria, Las Palmas, Spain

Received 5 May 2006; received in revised form 21 August 2006; accepted 1 September 2006
Available online 11 October 2006

Abstract

This paper deals with the study of power quality in an isolated system with high wind energy penetration level. An induction wind plant, a synchronous power plant and a network constitute the analysed system. The work focuses on studying the effect of mechanical power from wind on load voltage and network frequency fluctuations. A linear model for the complete system is proposed in order to use eigenfrequencies and Bode plots to carry out this study.

Keywords: Induction generators; Linear approximation; Power plants; Power quality; Synchronous generators; Wind power generation

1. Introduction

Nowadays, wind energy has an important impact in electrical networks, e.g. its growth rate has been continuously increasing over the last years, and wind power energy represents more than 5% of the Spanish electrical generation [1]. In isolated systems, the influence of wind energy is especially relevant. The Canary Islands are an example.

One of the typical problems of induction wind energy converters (WEC) is the variation of their delivered power, whose main cause is the random behaviour of wind. In addition, periodic fluctuations can appear in electrical power, which are mainly due to wind shear and tower shadow effect, as shown in measurements made by the authors [4,6,7] and other researchers [2,3,5].

In isolated networks with a large number of wind plants the oscillations mentioned above can be transmitted to the electrical loads and, thus, power quality is affected. In this paper a linear model is proposed to analyse the behaviour of these systems. This study can be carried out using tools such as eigenfrequencies and frequency response. The results are compared to those when the wind park is connected through a network to an infinite bus behind a reactance. This means that the network frequency is constant, which is equivalent to a power plant with an infinite inertia constant ($H=\infty$) [8,11].

2. Dynamic model of an induction WEC

The induction generator can be modelled as a voltage source $\underline{E}_\alpha$ behind the impedance $R_\alpha + \mathrm{j}X_\alpha$, as can be seen in Fig. 1. This dynamic model is defined by considering balanced operation and no stator electromagnetic dynamic effects (constant electromagnetic flux), and is known as the third order induction machine model [9,10].

The internal voltage $\underline{E}_\alpha$ can be derived from the following equation [9]:

$$\frac{\mathrm{d}\underline{E}_\alpha}{\mathrm{d}t} = -\mathrm{j}\omega_\mathrm{s} s \underline{E}_\alpha - \frac{1}{T'_0}(\underline{E}_\alpha - \mathrm{j}(X_0 - X_\alpha)\underline{I}_\alpha) \tag{1}$$

where ω_s is the synchronous frequency in rad/s (100π rad/s in Europe), s the slip, $\underline{I}_\alpha$ the stator current in p.u. and X_0, X_α and T'_0 are machine parameters in p.u.

The steady-state equation for the stator current is:

$$\underline{I}_\alpha = \frac{\underline{V}_\alpha - \underline{E}_\alpha}{R_\alpha + \mathrm{j}X_\alpha} \tag{2}$$

where $\underline{V}_\alpha$ is the external voltage of the induction machine in p.u., R_α and X_α are the parameters of the machine (see Appendix F) in p.u.

* Corresponding author. Tel.: +34 986 81 20 55; fax: +34 986 81 21 73.
E-mail address: afeijoo@uvigo.es (A.E. Feijóo).

0378-7796/$ – see front matter
doi:10.1016/j.epsr.2006.09.001

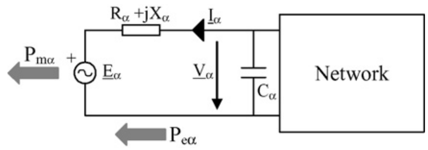

Fig. 1. Scheme of an induction generator in front of the network.

The electromechanical equation (see Appendix B) can be written as:

$$\frac{P_{m\alpha}}{1-s} - P_{e\alpha} = 2H_\alpha \frac{ds}{dt} \tag{3}$$

where $P_{m\alpha}$ is the WEC mechanical power ($P_{m\alpha} < 0$ for generation) in p.u., H_α the inertia constant in s and $P_{e\alpha}$ is the electrical power ($P_{e\alpha} < 0$ for generation) in p.u.

The electrical power in p.u., $P_{e\alpha}$, is calculated as:

$$P_{e\alpha} = \text{real}\left\{\underline{E}_\alpha \underline{I}_\alpha^*\right\} \tag{4}$$

In this paper, the WEC mechanical power $P_{m\alpha}(t)$ is represented with two components [11]:

$$P_{m\alpha}(t) = P_{m\alpha 0} + \Delta P_{m\alpha} \tag{5}$$

where $P_{m\alpha 0}$ represents the low frequency component of wind power, which is obtained from the mean value of the wind, defined by a Weibull or a Rayleigh distribution [12–14]. In this paper the $P_{m\alpha 0}$ component of mechanical power is assumed to be constant and $\Delta P_{m\alpha}$ is the power fluctuation with a frequency of about 1–2 Hz [2–4,6,7].

In order to make easier to study the power fluctuations influence on power quality, they are assumed to such as:

$$\Delta P_{m\alpha} = P_s \sin\theta(t) \tag{6}$$

where P_s is the amplitude of mechanical sinusoidal fluctuations in p.u. and $\theta(t)$ is the mechanical angle of the turbine in rad and is defined as:

$$\theta(t) = \theta_0 + \int_{t_0}^{t} (1 - s_0 + \Delta s)\omega_{pf}\, dt \approx \theta_0 + \omega_{pf} t \tag{7}$$

and θ_0 is the initial mechanical angle in rad, s_0 the initial slip of the induction generator, Δs equal to $s - s_0$ and ω_{pf} is the frequency of power fluctuations due to tower shadow effect in rad/s, which can be expressed as a function of the wind turbine rotational speed (Ω_r) by means of the following equation:

$$\omega_{pf} = 3\Omega_r = \frac{3\omega_s}{rp} \tag{8}$$

where r is the gearbox ratio and p is the number of pole pairs.

In this way, the expression for the power fluctuation can be written as:

$$\Delta P_{m\alpha} = P_s \sin(\omega_{pf} t + \theta_0). \tag{9}$$

3. Linear dynamic model of an induction wind park

The linear model for the induction machine is based on the following considerations [11,15]:

- The induction generator has an initial steady-state operating condition, defined by: $\underline{E}_{\alpha 0}$, $\underline{I}_{\alpha 0}$, $\underline{V}_{\alpha 0}$, s_0, P_{m0}.
- Small changes are: $\Delta\underline{E}_\alpha\, \Delta s \approx 0$, $\Delta s \ll s_0$, $\Delta\underline{E}_\alpha\, \Delta\underline{E}_\alpha^* \approx 0$, $\Delta\underline{E}_\alpha\, \Delta\underline{V}_\alpha^* \approx 0$ and $\sin\Delta\theta \approx 0$.

Eq. (1) can be linearized as:

$$\frac{d\Delta\underline{E}_\alpha}{dt} = -j\omega_s \underline{E}_{\alpha 0}\, \Delta s + \underline{z}'\, \Delta\underline{V}_\alpha - \underline{z}\, \Delta\underline{E}_\alpha \tag{10}$$

where

$$\underline{z} = v + jw = j\omega_s s_0 + \frac{1}{T_0'}\left(1 + j\frac{X_0 - X_\alpha}{R_\alpha + jX_\alpha}\right)$$

$$\underline{z}' = v' + jw' = \frac{1}{T_0'}\frac{X_0 - X_\alpha}{R_\alpha + jX_\alpha} j$$

In the same way, the mechanical Eq. (3) is:

$$h_\alpha \frac{d\Delta s}{dt} = \Delta P_{m\alpha} + \frac{P_{m\alpha 0}}{1 - s_0}\Delta s - (1 - s_0)\,\Delta P_{e\alpha} \tag{11}$$

where $h_\alpha = 2H_\alpha(1 - s_0)$

Finally, using Eqs. (2) and (4), electrical power can be expressed as:

$$\Delta P_{e\alpha} = g\,\Delta V_\alpha^r + m\,\Delta V_\alpha^m + e\,\Delta E_\alpha^r + f\,\Delta E_\alpha^m \tag{12}$$

where

$$\underline{y} = g + jm = \frac{\underline{E}_{\alpha 0}}{R_\alpha - jX_\alpha}$$

$$e = \text{real}\left\{\frac{\underline{V}_{\alpha 0}^* - E_{\alpha 0}^r / \underline{E}_{\alpha 0}}{R_\alpha - jX_\alpha}\right\}$$

$$f = \text{real}\left\{\frac{j\underline{V}_{\alpha 0}^* - E_{\alpha 0}^m / \underline{E}_{\alpha 0}}{R_\alpha - jX_\alpha}\right\}$$

Taking Eqs. (1)–(3), (11) and (12) into account, and the previous considerations:

$$\frac{d}{dt}\begin{bmatrix}\Delta E_\alpha^r\\ \Delta E_\alpha^m\\ \Delta s\end{bmatrix} = \mathbf{A}_\alpha \begin{bmatrix}\Delta E_\alpha^r\\ \Delta E_\alpha^m\\ \Delta s\end{bmatrix} + \mathbf{B}_{\alpha V_\alpha}\begin{bmatrix}\Delta V_\alpha^r\\ \Delta V_\alpha^m\end{bmatrix} + \mathbf{B}_{\alpha P}\,\Delta P_{m\alpha} \tag{13}$$

where

$$\mathbf{A}_\alpha = \begin{bmatrix} -v & w & \omega_s E_{\alpha 0}^m \\ -w & -v & -\omega_s E_{\alpha 0}^r \\ \dfrac{-e(1-s_0)}{h_\alpha} & \dfrac{-f(1-s_0)}{h_\alpha} & \dfrac{P_{m\alpha 0}}{((1-s_0)h_\alpha)} \end{bmatrix}$$

$$\mathbf{B}_{\alpha V_\alpha} = \begin{bmatrix} v' & -w' \\ w' & v' \\ \dfrac{-g(1-s_0)}{h_\alpha} & \dfrac{-m(1-s_0)}{h_\alpha} \end{bmatrix}$$

$$\mathbf{B}_{\alpha P} = \begin{bmatrix} 0 & 0 & \dfrac{1}{h_\alpha} \end{bmatrix}^T$$

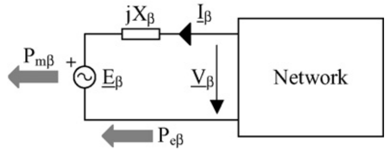

Fig. 2. Scheme of a synchronous generator in front of the network.

The parameters for Eq. (13) should be obtained by aggregating the different WEC's in the wind parks under consideration [17,18]. However, this task is not the purpose of this paper and the simple method has been used, consisting of assuming the wind parks as being constituted by machines with the parameters shown in Appendix F. So, the eigenvalues −7.91 and −4.10 ± 14.68j can be derived from Eq. (13) and their eigenfrequencies are represented in Fig. 4.

4. Linear dynamic model of a power plant

The aggregated synchronous generation of a power plant when it is formed by coherent synchronous generators can be modelled as a Thevenin equivalent voltage source $\underline{E}_\beta$, behind the transient reactance $\mathrm{j}X_\beta$, as can be seen in Fig. 2 [16].

The electromechanical equation for the plant formed by the synchronous generators is [10]:

$$P_{m\beta} - P_{e\beta} = -\frac{2H_\beta}{\omega_s}\frac{\mathrm{d}(\omega_\beta - \omega_s)}{\mathrm{d}t} \tag{14}$$

$$\frac{\mathrm{d}}{\mathrm{d}t}\delta_\beta = \omega_\beta - \omega_s \tag{15}$$

where δ_β is the angle of the internal voltage $\underline{E}_\beta$ in rad, ω_β the rotational speed of the synchronous machine in rad/s, ω_s the synchronous speed in rad/s, $P_{m\beta}$ the mechanical power in the power plant ($P_{m\beta} < 0$ for generation) in p.u., H_β the inertial constant in s and $P_{e\beta}$ the real electrical power ($P_{e\beta} < 0$ for generation) in p.u.

The electrical power $P_{e\beta}$ is calculated by:

$$P_{e\beta} = \mathrm{real}\left\{\underline{E}_\beta \underline{I}_\beta^*\right\} \tag{16}$$

where $\underline{I}_\beta$ is the stator current.

The stator current is:

$$\underline{I}_\beta = \frac{\underline{V}_\beta - \underline{E}_\beta}{\mathrm{j}X_\beta} \tag{17}$$

Taking the voltages in the polar form as:

$$\begin{aligned} \underline{V}_\beta &= V_\beta \angle \delta'_\beta \\ \underline{E}_\beta &= E_\beta \angle \delta_\beta = E_\beta \angle(\delta_\beta^{\mathrm{rel}} - \delta'_\beta) \end{aligned} \tag{18}$$

then, taking Eq. (17) into account, Eq. (16) can be written as:

$$P_{e\beta} = -\frac{E_\beta V_\beta}{X_\beta}\sin\delta_\beta^{\mathrm{rel}} \tag{19}$$

Consequently, the incremental dynamic model of the power plant, from an initial steady-state situation ($P_{m\beta 0} - P_{e\beta 0} = 0$; $\omega_{\beta 0} = \omega_s$; $\delta_{\beta 0}$; $E_{\beta 0}$) and assuming small changes, is:

$$\Delta P_{m\beta} - \Delta P_{e\beta} = -\frac{2H_\beta}{\omega_s}\frac{\mathrm{d}\Delta\omega_\beta}{\mathrm{d}t} \tag{20}$$

$$\Delta P_{e\beta} \approx \frac{\partial P_{e\beta 0}}{\partial E_\beta}\Delta E_\beta + \frac{\partial P_{e\beta 0}}{\partial V_\beta}\Delta V_\beta + \frac{\partial P_{e\beta 0}}{\partial \delta_\beta^{\mathrm{rel}}}\Delta\delta_\beta^{\mathrm{rel}} \tag{21}$$

The power can be expressed as:

$$\Delta P_{e\beta} = -p\,\Delta E_\beta - q\,\Delta V_\beta - dE_{\beta 0}\,\Delta\delta_\beta - d' V_{\beta 0}\,\Delta\delta'_\beta \tag{22}$$

where

$$p = \frac{V_{\beta 0}\sin\delta_{\beta 0}^{\mathrm{rel}}}{X_\beta}$$

$$q = \frac{E_{\beta 0}\sin\delta_{\beta 0}^{\mathrm{rel}}}{X_\beta}$$

$$d = \frac{V_{\beta 0}\cos\delta_{\beta 0}^{\mathrm{rel}}}{X_\beta}$$

$$d' = \frac{-E_{\beta 0}\cos\delta_{\beta 0}^{\mathrm{rel}}}{X_\beta}$$

Machine equations in matrix form are:

$$\frac{\mathrm{d}}{\mathrm{d}t}\begin{bmatrix}\Delta\omega_\beta \\ E_{\beta 0}\,\Delta\delta_\beta\end{bmatrix} = \begin{bmatrix} 0 & \dfrac{-d}{h_\beta} \\ E_{\beta 0} & 0 \end{bmatrix}\begin{bmatrix}\Delta\omega_\beta \\ E_{\beta 0}\,\Delta\delta_\beta\end{bmatrix} + \begin{bmatrix} \dfrac{-q}{h_\beta} & \dfrac{-d'}{h_\beta} & \dfrac{-p}{h_\beta} & \dfrac{-1}{h_\beta} \\ 0 & 0 & 0 & 0 \end{bmatrix}\begin{bmatrix}\Delta V_\beta \\ V_{\beta 0}\,\Delta\delta'_\beta \\ \Delta E_\beta \\ \Delta P_{m\beta}\end{bmatrix} \tag{23}$$

where $h_\beta = 2H_\beta/\omega_s$.

The system depicted in Eq. (23) has two imaginary eigenvalues whose frequency depends on inertia constant H_β. In Appendix F, the relationship between nominal power $P_{\beta,\mathrm{nom}}$ and inertia constant H_β is shown [16]. Using the parameters in Appendix F, the evolution of the eigenfrequencies shown in Fig. 4 can be obtained.

In synchronous generation there are two automatic control systems: P–ω and Q–V regulator. Their configurations are shown in Appendix E and their parameters are in Appendix F [16].

5. Linear dynamic model of a power system with a wind park and a power plant

An induction wind park, a conventional power plant and an electrical network constitute the complete system (see Fig. 3). All the parameters of the network are in p.u. quantities with the base values shown in Appendix F. Transformers are not represented but they have been included and modelled by means of their correspondent short-circuit impedances.

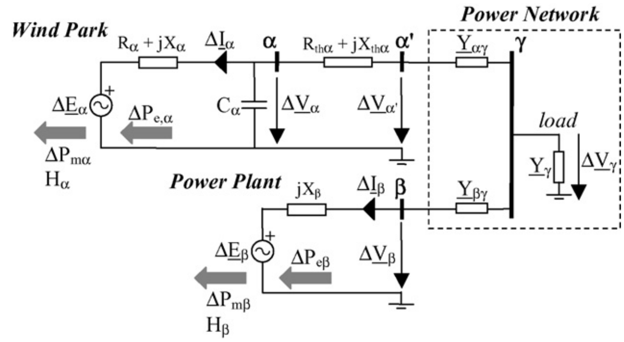

Fig. 3. Scheme of the network.

In order to obtain the complete linear model of the system shown in Fig. 3, nodal analysis is applied, and the result is:

$$\underline{Y}\begin{bmatrix}\Delta\underline{V}_\alpha\\ \Delta\underline{V}_{\alpha'}\\ \Delta\underline{V}_\beta\\ \Delta\underline{V}_\gamma\end{bmatrix}=\begin{bmatrix}\underline{Y}_\alpha\,\Delta\underline{E}_\alpha\\ 0\\ \underline{Y}_\beta\,\Delta\underline{E}_\beta\\ 0\end{bmatrix} \tag{24}$$

where

$$\underline{\mathbf{Y}}=\begin{bmatrix}\underline{Y}_\alpha+\mathrm{j}\omega_s C_\alpha+\underline{Y}_{\text{th}\alpha} & -\underline{Y}_{\text{th}\alpha} & 0 & 0\\ -\underline{Y}_{\text{th}\alpha} & \underline{Y}_{\text{th}\alpha}+\underline{Y}_{\alpha\gamma} & 0 & -\underline{Y}_{\alpha\gamma}\\ 0 & 0 & \underline{Y}_\beta+\underline{Y}_{\beta\gamma} & -\underline{Y}_{\beta\gamma}\\ 0 & -\underline{Y}_{\alpha\gamma} & -\underline{Y}_{\beta\gamma} & \underline{Y}_\gamma+\underline{Y}_{\beta\gamma}+\underline{Y}_{\alpha\gamma}\end{bmatrix} \tag{25}$$

and

$$\underline{Y}_\beta=\frac{1}{\mathrm{j}X_\beta}$$

$$\underline{Y}_\alpha=(R_\alpha+\mathrm{j}X_\alpha)^{-1}$$

$$\underline{Y}_{\text{th}\alpha}=(R_{\text{th}\alpha}+\mathrm{j}X_{\text{th}\alpha})^{-1}$$

So, the relationship between the network and the internal voltages is:

$$\begin{bmatrix}\Delta\underline{V}_\alpha\\ \Delta\underline{V}_{\alpha'}\\ \Delta\underline{V}_\beta\\ \Delta\underline{V}_\gamma\end{bmatrix}=\underline{\mathbf{K}}\begin{bmatrix}\Delta\underline{E}_\alpha\\ 0\\ \Delta\underline{E}_\beta\\ 0\end{bmatrix} \tag{26}$$

where

$$\underline{\mathbf{K}}=\begin{cases}\underline{K}_{i,1}=\underline{Y}_{i,1}^{-1}\underline{Y}_\alpha, & i=1,\ldots,4\\ \underline{K}_{i,3}=\underline{Y}_{i,3}^{-1}\underline{Y}_\beta, & i=1,\ldots,4\\ \underline{K}_{i,j}=\underline{Y}_{i,j}^{-1}, & i=1,\ldots,4,\ j=\{2,4\}\end{cases}$$

Using the polar form for the synchronous machine and the complex form for the induction one, Eq. (26) results in:

$$\begin{bmatrix}\Delta V_\alpha^{\mathrm{r}}\\ \Delta V_\alpha^{\mathrm{m}}\end{bmatrix}=\mathbf{K}_{\alpha\alpha}\begin{bmatrix}\Delta E_\alpha^{\mathrm{r}}\\ \Delta E_\alpha^{\mathrm{m}}\end{bmatrix}+\mathbf{K}_{\alpha\beta}\begin{bmatrix}\Delta E_\beta\\ E_{\beta0}\,\Delta\delta_\beta\end{bmatrix} \tag{27}$$

$$\begin{bmatrix}\Delta V_\beta\\ V_{\beta0}\,\Delta\delta'_\beta\end{bmatrix}=\mathbf{K}_{\beta\alpha}\begin{bmatrix}\Delta E_\alpha^{\mathrm{r}}\\ \Delta E_\alpha^{\mathrm{m}}\end{bmatrix}+\mathbf{K}_{\beta\beta}\begin{bmatrix}\Delta E_\beta\\ E_{\beta0}\,\Delta\delta_\beta\end{bmatrix} \tag{28}$$

where

$$\mathbf{K}_{\alpha\alpha}=\begin{bmatrix}K_{11}^{\mathrm{r}} & -K_{11}^{\mathrm{m}}\\ K_{11}^{\mathrm{m}} & K_{11}^{\mathrm{r}}\end{bmatrix}$$

$$\mathbf{K}_{\alpha\beta}=\begin{bmatrix}K_{13}^{\mathrm{r}} & -K_{13}^{\mathrm{m}}\\ K_{13}^{\mathrm{m}} & K_{13}^{\mathrm{r}}\end{bmatrix}\mathbf{T}_{E_\beta}$$

$$\mathbf{K}_{\beta\alpha}=\mathbf{T}_{V_\beta}^{\mathrm{T}}\begin{bmatrix}K_{31}^{\mathrm{r}} & -K_{31}^{\mathrm{m}}\\ K_{31}^{\mathrm{m}} & K_{31}^{\mathrm{r}}\end{bmatrix}$$

$$\mathbf{K}_{\beta\beta}=\mathbf{T}_{V_\beta}^{\mathrm{T}}\begin{bmatrix}K_{33}^{\mathrm{r}} & -K_{33}^{\mathrm{m}}\\ K_{33}^{\mathrm{m}} & K_{33}^{\mathrm{r}}\end{bmatrix}\mathbf{T}_{E_\beta}$$

$\mathbf{T}_{V_\beta}$ and $\mathbf{T}_{E_\beta}$ are the transformation matrix for $\underline{V}_\beta$ and $\underline{E}_\beta$ (see Appendix C)

5.1. Induction machine

Using nodal Eqs. (27) and (28) with Eq. (13), the equation for the induction machine can now be written as:

$$\frac{\mathrm{d}}{\mathrm{d}t}\begin{bmatrix}\Delta E_\alpha^{\mathrm{r}}\\ \Delta E_\alpha^{\mathrm{m}}\\ \Delta s\end{bmatrix}=\mathbf{A}_\alpha\begin{bmatrix}\Delta E_\alpha^{\mathrm{r}}\\ \Delta E_\alpha^{\mathrm{m}}\\ \Delta s\end{bmatrix}+\mathbf{B}_{\alpha E_\alpha}\begin{bmatrix}\Delta E_\alpha^{\mathrm{r}}\\ \Delta E_\alpha^{\mathrm{m}}\end{bmatrix}+\mathbf{B}_{\alpha E_\beta}\begin{bmatrix}\Delta E_\beta\\ E_{\beta0}\,\Delta\delta_\beta\end{bmatrix}+\mathbf{B}_{\alpha P}\Delta P_{\mathrm{m}\alpha} \tag{29}$$

where

$$\mathbf{B}_{\alpha E_\alpha}=\mathbf{B}_{\alpha V_\alpha}\mathbf{K}_{\alpha\alpha}$$

$$\mathbf{B}_{\alpha E_\beta}=\mathbf{B}_{\alpha V_\alpha}\mathbf{B}_{\alpha\beta}$$

Eq. (29) can be written as:

$$\frac{\mathrm{d}}{\mathrm{d}t}\begin{bmatrix}\Delta E_\alpha^{\mathrm{r}}\\ \Delta E_\alpha^{\mathrm{m}}\\ \Delta s\end{bmatrix}=\mathbf{A}'_\alpha\begin{bmatrix}\Delta E_\alpha^{\mathrm{r}}\\ \Delta E_\alpha^{\mathrm{m}}\\ \Delta s\end{bmatrix}+\mathbf{B}'_\alpha\begin{bmatrix}\Delta E_\beta\\ E_{\beta0}\,\Delta\delta_\beta\\ \Delta P_{\mathrm{m}\alpha}\end{bmatrix} \tag{30}$$

where

$$\mathbf{A}'_\alpha=\begin{bmatrix}-v+B_{\alpha E_\alpha 11} & w+B_{\alpha E_\alpha 12} & \omega_s E_{\alpha0}^{\mathrm{m}}\\ -w+B_{\alpha E_\alpha 21} & -v+B_{\alpha E_\alpha 22} & -\omega_s E_{\alpha0}^{\mathrm{r}}\\ -e\dfrac{1-s_0}{h_\alpha}+B_{\alpha E_\alpha 31} & -f\dfrac{1-s_0}{h_\alpha}+B_{\alpha E_\alpha 32} & \dfrac{P_{\mathrm{m}\alpha0}}{(1-s_0)h_\alpha}\end{bmatrix}$$

$$\mathbf{B}'_\alpha=\begin{bmatrix}\mathbf{B}_{\alpha E_\beta} & \mathbf{B}_{\alpha P}\end{bmatrix}$$

The output for this system is formed by the state variables: $\Delta E_\alpha^{\mathrm{r}}$, $\Delta E_\alpha^{\mathrm{m}}$ and Δs.

Fig. 4 shows the eigenfrequencies of the system depicted by Eq. (30) with the parameters in Appendix F.

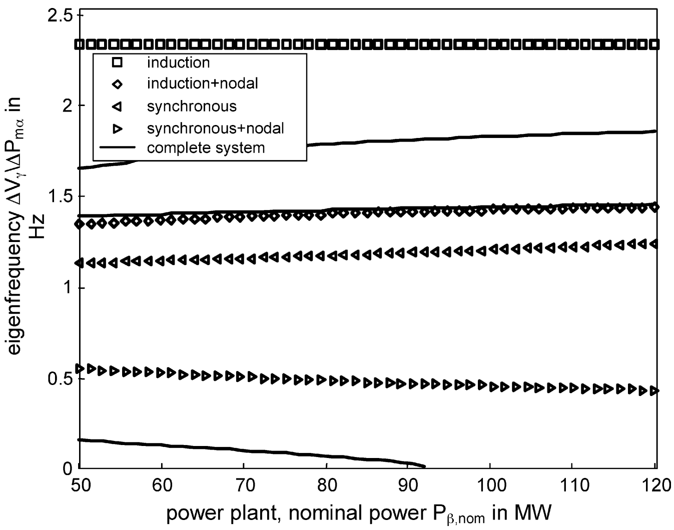

Fig. 4. Eigenfrequency values in a system formed by a 35 MVA wind park.

5.2. Synchronous machine

Eq. (28) can be written as:

$$\begin{aligned} \Delta V_\beta &= K_{\beta\alpha 11}\,\Delta E^{\mathrm{r}}_\alpha + K_{\beta\alpha 12}\,\Delta E^{\mathrm{m}}_\alpha + K_{\beta\beta 11}\,\Delta E_\beta \\ &\quad + K_{\beta\beta 12} E_{\beta 0}\,\Delta\delta_\beta \\ V_{\beta 0}\,\Delta\delta'_\beta &= K_{\beta\alpha 21}\,\Delta E^{\mathrm{r}}_\alpha + K_{\beta\alpha 22}\,\Delta E^{\mathrm{m}}_\alpha + K_{\beta\beta 21}\,\Delta E_\beta \\ &\quad + K_{\beta\beta 22} E_{\beta 0}\,\Delta\delta_\beta \end{aligned} \tag{31}$$

Using nodal Eq. (31) in Eq. (23), synchronous machine equations can be written as:

$$\frac{\mathrm{d}}{\mathrm{d}t}\begin{bmatrix} \Delta\omega_\beta \\ E_{\beta 0}\,\Delta\delta^{\mathrm{rel}}_\beta \end{bmatrix} = \mathbf{A}'_\beta \begin{bmatrix} \Delta\omega_\beta \\ E_{\beta 0}\,\Delta\delta^{\mathrm{rel}}_\beta \end{bmatrix} + \mathbf{B}'_\beta \begin{bmatrix} \Delta E^{\mathrm{r}}_\alpha \\ \Delta E^{\mathrm{m}}_\alpha \\ \Delta E_\beta \\ \Delta P_{\mathrm{m}\beta} \end{bmatrix} \tag{32}$$

$$\begin{bmatrix} \Delta\omega_\beta \\ E_{\beta 0}\,\Delta\delta_\beta \end{bmatrix} = \mathbf{C}'_\beta \begin{bmatrix} \Delta\omega_\beta \\ E_{\beta 0}\,\Delta\delta_\beta \end{bmatrix} + \mathbf{D}'_\beta \begin{bmatrix} \Delta E^{\mathrm{r}}_\alpha \\ \Delta E^{\mathrm{m}}_\alpha \\ \Delta E_\beta \\ \Delta P_{\mathrm{m}\beta} \end{bmatrix} \tag{33}$$

where

$$\mathbf{A}'_\beta = \begin{bmatrix} 0 & k_1 \\ E_{\beta 0} & 0 \end{bmatrix}$$

$$\mathbf{B}'_\beta = \begin{bmatrix} k_2 & k_3 & k_4 & \dfrac{-1}{h_\beta} \\ 0 & 0 & 0 & 0 \end{bmatrix}$$

$$\mathbf{C}'_\beta = \begin{bmatrix} 1 & 0 \\ 0 & 1 \end{bmatrix}$$

$$\mathbf{D}'_\beta = \begin{bmatrix} 0 & 0 & 0 & 0 \\ 0 & 0 & 0 & 0 \end{bmatrix}$$

and

$$k_1 = \frac{-qK_{\beta\beta 12} - d - d'K_{\beta\beta 22}}{h_\beta}$$

$$k_2 = \frac{-qK_{\beta\alpha 11} - d'K_{\beta\alpha 12}}{h_\beta}$$

$$k_3 = \frac{-qK_{\beta\alpha 12} - d'K_{\beta\alpha 22}}{h_\beta}$$

$$k_4 = \frac{-p - qK_{\beta\beta 11} - d'K_{\beta\beta 12}}{h_\beta}$$

Eigenvalues of Eq. (32) with the parameters in Appendix F are shown in Fig. 4.

6. Linear model for the complete system

The models presented in the previous paragraphs can be connected as shown in Fig. 5, in order to model the complete system. The behaviour of this system will be studied choosing mechanical power $\Delta P_{\mathrm{m}\alpha}$ as input and with the following outputs: voltage ΔV_γ and rotational speed $\Delta\omega_\beta$. In this way, the influence of the wind park on the variations on load voltage and frequency deviation can be studied.

The linearized equations of a system formed by a 150 MVA power plant and a 35 MVA induction wind park (see Appendix F) have been simulated with SIMULINK [20]. These results have been compared with those obtained using the commercial program SIMPOW [21], where electrical machines are represented in a *d–q* frame. There is a good agreement between the two simulations as can be seen in Fig. 6. In the same way, a comparison between frequency responses of the linear system (Bode plot) and the in *d–q* reference is shown in Fig. 7.

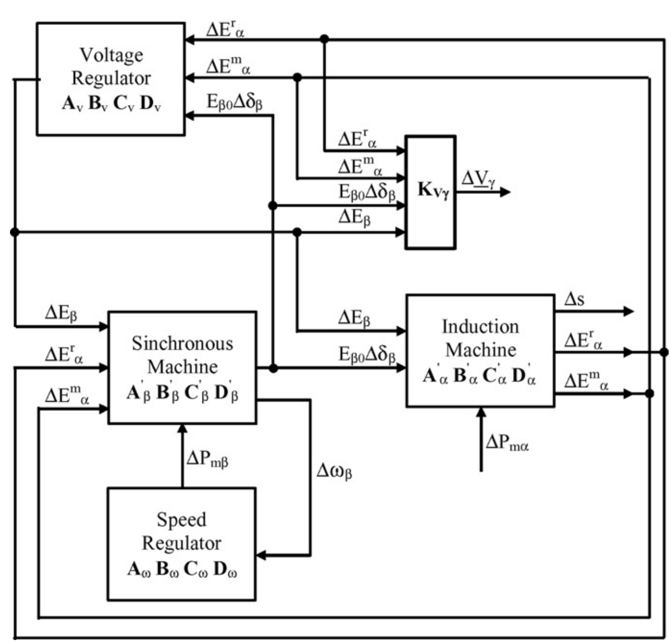

Fig. 5. Block diagram of the complete system.

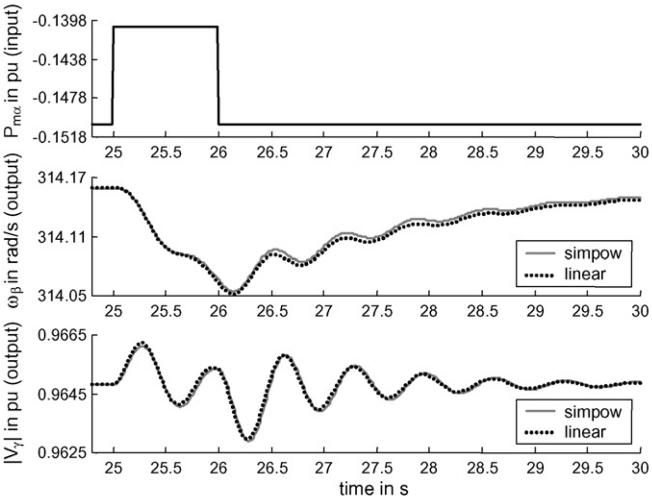

Fig. 6. Results from simulations with SIMPOW (*dq* representation) and linear model.

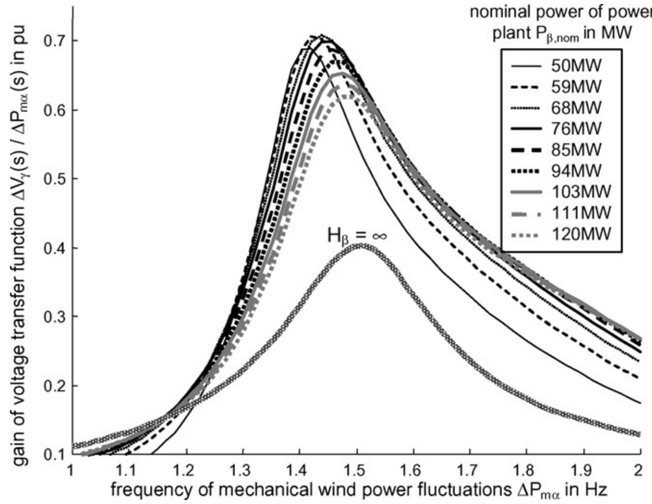

Fig. 8. Evolution of the Bode plot magnitude for the voltage transfer function $\Delta V_\gamma(s)/\Delta P_{m\alpha}(s)$.

Once the linear model has been obtained, the transfer functions $\Delta V_\gamma(s)/\Delta P_{m\alpha}(s)$ and $\Delta\omega_\beta(s)/\Delta P_{m\alpha}(s)$ can be computed. For a system formed by a 150 MVA power plant and a 35 MVA induction wind park (see Appendix F), these functions have 11 poles and the main eigenfrequencies can be seen in Fig. 4.

In order to illustrate the impact of the WEC mechanical power fluctuations in load voltage ΔV_γ, the magnitude of the Bode plot for $\Delta V_\gamma(s)/\Delta P_{m\alpha}(s)$ between 1 and 2 Hz is shown in Fig. 8. As can be seen, the amplitude of voltage fluctuations increases when the nominal power of a power plant decreases. This effect is greater when compared with a power plant modelled as infinite bus behind a reactance ($H_\beta = \infty$).

When a similar study is carried out with the speed transfer function $\Delta\omega_\beta(s)/\Delta P_{m\alpha}(s)$, the results shown in Fig. 9 are achieved. These values in Bode plot are much lower than those for $\Delta V_\gamma(s)/\Delta P_{m\alpha}(s)$. For example, the maximum value for $\Delta V_\gamma(s)/\Delta P_{m\alpha}(s)$ is 0.7 and the value corresponding to $\Delta\omega_\beta(s)/\Delta P_{m\alpha}(s)$ is 15 rad/s/p.u. or 0.048 p.u./p.u. The relationship between nominal power of the power plant and the peak for the fluctuation magnitude shown in Figs. 10 and 11 reflects more clearly this behaviour.

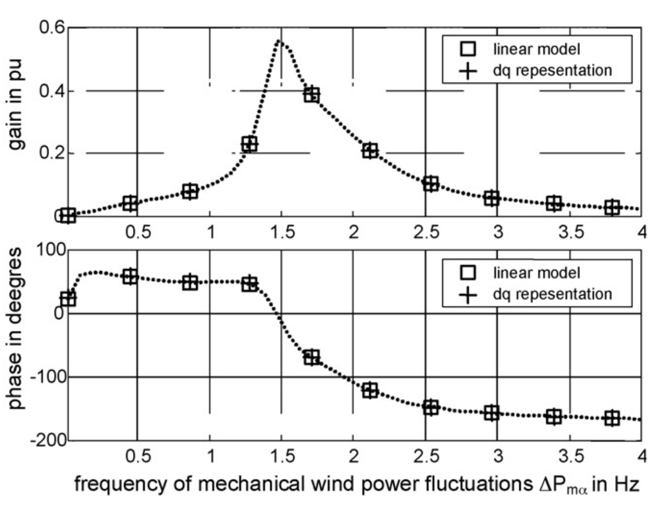

Fig. 7. Frequency response of complete system taking mechanical power $P_{m\alpha}$ as input and load voltage V_γ as output in a system formed by a 150 MVA power plant and a 35 MVA wind park.

7. Results

Assuming that voltage variations are much higher than the speed variations, only the behaviour of the load voltage has been analysed in this section.

And assuming that the oscillatory power defined in Eq. (9) is the input for the complete system, the expression for voltage V_γ and speed ω_β, can be written as:

$$\Delta V_\gamma = V_s \sin(\omega_{pf} t + \theta_0'') \tag{34}$$

where V_s and θ_0'' represent the amplitude and initial phase for the oscillations in voltage.

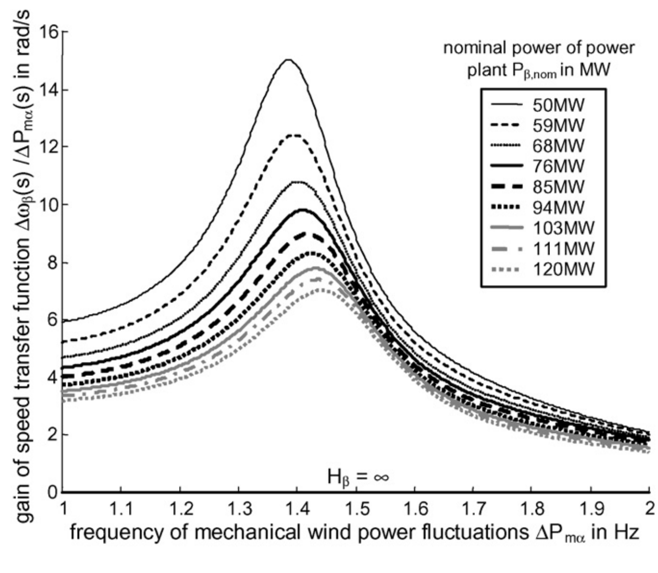

Fig. 9. Evolution of the Bode plot magnitude for the speed transfer function $\Delta\omega_\beta(s)/\Delta P_{m\alpha}(s)$.

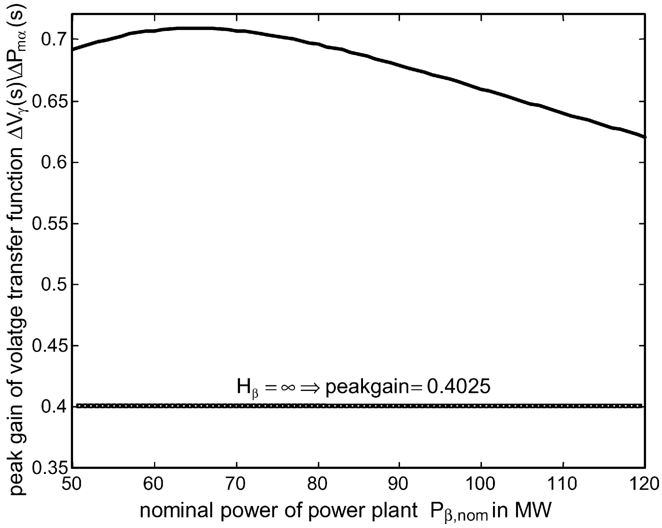

Fig. 10. Evolution of the peak magnitude values for the voltage transfer function $\Delta V_\gamma(s)/\Delta P_{m\alpha}(s)$.

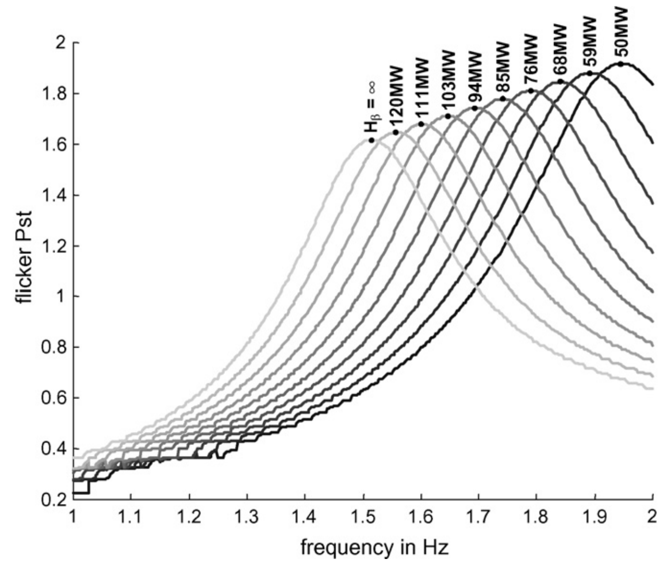

Fig. 12. Evolution of the flicker (Pst) related to load voltage variations.

Values for the amplitudes and phases depicted above can be obtained from the transfer functions evaluated at $j\Omega_s$, so:

$$V_{\angle\theta_0''} = \left.\frac{\Delta V_\gamma(s)}{\Delta P_{m\alpha}(s)}\right|_{s=j\Omega_s} \quad (35)$$

where considering Eq. (9) $\Delta P_{m\alpha}(j\omega_f) = P_s\angle\theta_0$

As shown in Fig. 8, the value for voltage and speed oscillations depends on the synchronous machines nominal powers and also on the frequency Ω_s of the mechanical power oscillations.

The results shown in Fig. 10 show that the peak of magnitude is achieved for values in the neighbourhood of tower shadow effect (between 1 and 2 Hz), for a system with the parameters given in Appendix F. As this effect is one of the most important perturbations in wind parks, this behaviour can lead to high flicker values relating load voltage variations. In Fig. 12 the results of flicker computation are shown [22], by assuming a pessimistic situation where the power oscillation due to tower shadow has an amplitude of 20% [2,3] with respect to the nominal power of the wind park.

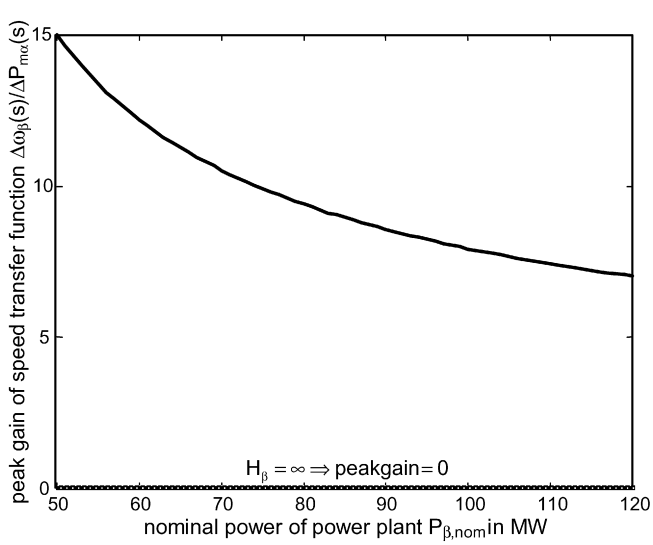

Fig. 11. Evolution of the peak magnitude values for the speed transfer function $\Delta\omega_\beta(s)/\Delta P_{m\alpha}(s)$.

8. Conclusion

In this paper, a linear model for the behaviour of a power system with high wind energy penetration is presented. Once the model has been developed it has been used to study the behaviour of the voltage in the load and the frequency in the network when the wind park introduces variations on power.

One of the main perturbations associated with a wind park is given by the tower shadow effect. The oscillation frequency of the electrical power delivered by the wind park in these conditions has a frequency between 1 and 2 Hz. This paper presents a method to evaluate the impact (flicker, voltage variations and frequency deviations) of wind parks on networks under these conditions. This analysis is more relevant in isolated networks, as shown in the results.

Acknowledgment

The financial support given by the Ministerio de Ciencia y Tecnología under the contract DPI2002-02770 is gratefully acknowledged by the authors.

Appendix A. Notation of constants and variables

$\underline{E}$	complex number
E	modulus of $\underline{E}$
E^r, E^m	real or imaginary part of $\underline{E}$
A, **a**	matrix or vector
A, a	constant or parameter
$A_{i,j}$, a_i	elements of matrix **A** or vector **a**

Appendix B. Electromechanical equation of induction machines

The electromechanical equation of an induction machine can be written as [10]:

$$T_{\mathrm{m}} - T_{\mathrm{e}} = -J\,\frac{\mathrm{d}\Omega}{\mathrm{d}t} \tag{36}$$

where T_{m} and T_{e} are the mechanical and electromagnetic torque, respectively, in N m ($T_{\mathrm{m}} < 0$ and $T_{\mathrm{e}} < 0$ for generation), J the inertia moment in N m s^2 and Ω is the rotor speed in rad/s.

In this equation electrical power (P_{e}) and mechanical power (P_{m}) can be included if the following relationships are taken into account:

$$\Omega = (1 - s)\Omega_{\mathrm{s}} \tag{37}$$

$$P_{\mathrm{m}} = T_{\mathrm{m}}\Omega = T_{\mathrm{m}}(1 - s)\Omega_{\mathrm{s}} \tag{38}$$

$$P_{\mathrm{e}} = T_{\mathrm{e}}\Omega_{\mathrm{s}} \tag{39}$$

where Ω and Ω_{s} are the rotor and synchronous speeds, respectively. In this way, Eq. (36) can be written as:

$$\frac{P_{\mathrm{m}}}{1 - s} - P_{\mathrm{e}} = J\Omega_{\mathrm{s}}^2\,\frac{\mathrm{d}s}{\mathrm{d}t} \tag{40}$$

And using p.u. values:

$$\frac{P_{\mathrm{m}}}{1 - s} - P_{\mathrm{e}} = 2H\,\frac{\mathrm{d}s}{\mathrm{d}t} \tag{41}$$

Appendix C. Transformation from complex to polar

In this appendix the transformation between the complex and polar form is shown. This transformation is applied to the following voltage represented in its complex form:

$$\underline{V}_{\varepsilon} = V_{\varepsilon}^{\mathrm{r}} + \mathrm{j}V_{\varepsilon}^{\mathrm{m}} = V_{\varepsilon}(\cos\,\delta_{\varepsilon} + \mathrm{j}\,\sin\,\delta_{\varepsilon}) \tag{42}$$

By applying the Taylor equation, Eq. (42) can be written as:

$$\Delta\underline{V}_{\varepsilon} \approx \frac{\partial \underline{V}_{\varepsilon}}{\partial V_{\varepsilon}}\,\Delta V_{\varepsilon} + \frac{\partial \underline{V}_{\varepsilon}}{\partial \delta_{\varepsilon}}\,\Delta\delta_{\varepsilon} \tag{43}$$

where $\Delta\underline{V}_{\varepsilon} = \underline{V}_{\varepsilon} - \underline{V}_{\varepsilon 0}$. In this way, the complex values can be given as a function of polar components:

$$\begin{aligned}\Delta\underline{V}_{\varepsilon} &= \cos\,\delta_{\varepsilon 0}\,\Delta V_{\varepsilon} - \sin\,\delta_{\varepsilon 0} V_{\varepsilon 0}\,\Delta\delta_{\varepsilon}\\ &\quad + \mathrm{j}(\sin\,\delta_{\varepsilon 0}\,\Delta V_{\varepsilon} + \cos\,\delta_{\varepsilon 0} V_{\varepsilon 0}\,\Delta\delta_{\varepsilon})\end{aligned} \tag{44}$$

where $\underline{V}_{\varepsilon 0} = V_{\varepsilon 0}\angle\theta_{\varepsilon 0}$

The above expression can be written in matrix form:

$$\begin{bmatrix}\Delta V_{\varepsilon}^{\mathrm{r}}\\ \Delta V_{\varepsilon}^{\mathrm{m}}\end{bmatrix} = \mathbf{T}_{V_{\varepsilon}}\begin{bmatrix}\Delta V_{\varepsilon}\\ V_{\varepsilon 0}\,\Delta\delta_{\varepsilon}\end{bmatrix} \tag{45}$$

where transformation matrix $\mathbf{T}_{V_{\varepsilon}}$ is Hermitian ($\mathbf{T}_{V_{\varepsilon}}^{-1} = \mathbf{T}_{V_{\varepsilon}}^{\mathrm{T}}$) and can be written as:

$$\mathbf{T}_{V_{\varepsilon}} = \begin{bmatrix}\cos\,\delta_{\varepsilon 0} & -\sin\,\delta_{\varepsilon 0}\\ \sin\,\delta_{\varepsilon 0} & \cos\,\delta_{\varepsilon 0}\end{bmatrix} \tag{46}$$

Appendix D. Network voltages

The relationship between the internal voltages ($\underline{E}_{\alpha}$ and $\underline{E}_{\beta}$) and the network voltage $\underline{V}_{\gamma}$ is:

$$\begin{aligned}\begin{bmatrix}\Delta V_{\gamma}\\ V_{\gamma 0}\,\Delta\delta_{\gamma}\end{bmatrix} &= \mathbf{K}_{\gamma\alpha}\begin{bmatrix}\Delta E_{\alpha}^{\mathrm{r}}\\ \Delta E_{\alpha}^{\mathrm{m}}\end{bmatrix} + \mathbf{K}_{\gamma\beta}\begin{bmatrix}\Delta E_{\beta}\\ E_{\beta 0}\,\Delta\delta_{\beta}\end{bmatrix}\\ &= \mathbf{K}_{V_{\gamma}}\begin{bmatrix}\Delta E_{\alpha}^{\mathrm{r}}\\ \Delta E_{\alpha}^{\mathrm{m}}\\ \Delta E_{\beta}\\ E_{\beta 0}\,\Delta\delta_{\beta}\end{bmatrix}\end{aligned} \tag{47}$$

where

$$\mathbf{K}_{\gamma\alpha} = \mathbf{T}_{V_{\gamma}}^{\mathrm{T}}\begin{bmatrix}K_{41}^{\mathrm{r}} & -K_{41}^{\mathrm{m}}\\ K_{41}^{\mathrm{m}} & K_{41}^{\mathrm{r}}\end{bmatrix}$$

$$\mathbf{K}_{\gamma\beta} = \mathbf{T}_{V_{\gamma}}^{\mathrm{T}}\begin{bmatrix}K_{43}^{\mathrm{r}} & -K_{43}^{\mathrm{m}}\\ K_{43}^{\mathrm{m}} & K_{43}^{\mathrm{r}}\end{bmatrix}\mathbf{T}_{E_{\beta}}$$

$$\mathbf{K}_{V_{\gamma}} = \left[\mathbf{K}_{\gamma\alpha}|\mathbf{K}_{\gamma\beta}\right]$$

Appendix E. *P–F* and *Q–V* regulators for the synchronous machines

In this paper, a steam turbine and governor model have been used to represent the speed regulator of synchronous machines [19]. A block diagram is shown in Fig. 13, and its equation can be written as:

$$\frac{\mathrm{d}}{\mathrm{d}t}\begin{bmatrix}\Delta P_{\mathrm{m}\beta}\\ \Delta x_1\\ \Delta x_2\end{bmatrix} = \mathbf{A}_{\omega}\begin{bmatrix}\Delta P_{\mathrm{m}\beta}\\ \Delta x_1\\ \Delta x_2\end{bmatrix} + \mathbf{B}_{\omega}\,\Delta\omega_{\beta} \tag{48}$$

where Δx_1, Δx_2 and Δx_3 are state variables

$$\mathbf{A}_{\omega} = \begin{bmatrix}0 & 1 & 0\\ 0 & 0 & 1\\ -a_3 & -a_2 & -a_1\end{bmatrix}$$

$$\mathbf{B}_{\omega} = \begin{bmatrix}0\\ b_2\\ b_3 - a_1 b_2\end{bmatrix}$$

$$a_1 = \frac{T_1 T_3 + T_1 T_t + T_3 T_t}{T_1 T_3 T_t}$$

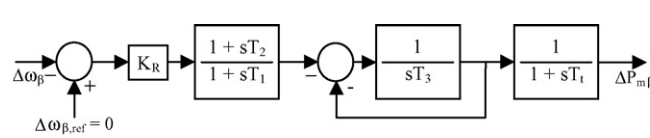

Fig. 13. Block diagram of speed controller.

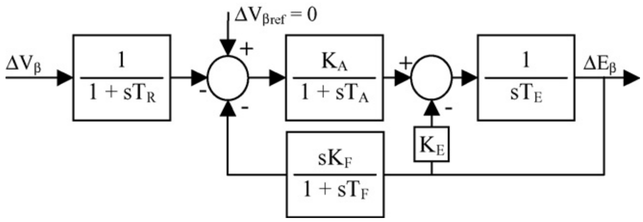

Fig. 14. Block diagram of voltage controller.

$$a_2 = \frac{T_1 + T_3 + T_t}{T_1 T_3 T_t}$$

$$a_3 = \frac{1}{T_1 T_3 T_t}$$

$$b_2 = \frac{-K_R T_2}{T_1 T_3 T_t}$$

$$b_3 = \frac{-K_R}{T_1 T_3 T_t}$$

In order to model the voltage regulator (see Fig. 14), an IEEE type DC1 exciter has been used [16], and its equation can be written:

$$\frac{\mathrm{d}}{\mathrm{d}t}\begin{bmatrix}\Delta E_\beta \\ \Delta y_1 \\ \Delta y_2 \\ \Delta y_3\end{bmatrix} = \mathbf{A}_v \begin{bmatrix}\Delta E_\beta \\ \Delta y_1 \\ \Delta y_2 \\ \Delta y_3\end{bmatrix} + \mathbf{B}_v\, \Delta V_\beta \tag{49}$$

$$\frac{\mathrm{d}}{\mathrm{d}t}\begin{bmatrix}\Delta E_\beta \\ \Delta y_1 \\ \Delta y_2 \\ \Delta y_3\end{bmatrix} = \begin{bmatrix} 0 & 1 & 0 & 0 \\ 0 & 0 & 1 & 0 \\ 0 & 0 & 0 & 1 \\ -a'_4 & -a'_3 & -a'_2 & -a'_1 \end{bmatrix}\begin{bmatrix}\Delta E_\beta \\ \Delta y_1 \\ \Delta y_2 \\ \Delta y_3\end{bmatrix} + \begin{bmatrix}0 \\ 0 \\ b'_3 \\ b''_4\end{bmatrix} \Delta V_\beta \tag{50}$$

where

$$K'_A = \frac{K_A}{K_E}; \qquad T'_E = \frac{T_E}{K_E}$$

$$a'_1 = \frac{T_A T_F T'_E + T_A T_R T'_E + T_A T_F T_R + T_F T_R T'_E}{T_A T'_E T_F T_R}$$

$$a'_2 = \frac{T_A T'_E + T_A T_F + T'_E T_F + T_A T_R + T'_E T_R + T_F T_R + K_F K'_A T_R}{T_A T'_E T_F T_R}$$

$$a'_3 = \frac{T_A + T'_E + T_F + T_R + K_F K'_A}{T_A T'_E T_F T_R}$$

$$a'_4 = \frac{K_E}{T_A T'_E T_F T_R}$$

$$b'_3 = \frac{-K'_A}{T_A T'_E T_R}$$

$$b''_4 = \frac{-K'_A}{T_A T'_E T_R T_F - a'_1 b'_3}$$

Using Eq. (31) state equations can be written as:

$$\frac{\mathrm{d}}{\mathrm{d}t}\begin{bmatrix}\Delta E_\beta \\ \Delta y_1 \\ \Delta y_2 \\ \Delta y_3\end{bmatrix} = \mathbf{A}_V \begin{bmatrix}\Delta E_\beta \\ \Delta y_1 \\ \Delta y_2 \\ \Delta y_3\end{bmatrix} + \mathbf{B}_V \begin{bmatrix}\Delta E^{\mathrm{r}}_\alpha \\ \Delta E^{\mathrm{m}}_\alpha \\ E_{\beta 0}\,\Delta\delta_\beta\end{bmatrix} \tag{51}$$

where Δy_1, Δy_2 and Δy_3 are state variables

$$\mathbf{A}_V = \begin{bmatrix} 0 & 1 & 0 & 0 \\ 0 & 0 & 1 & 0 \\ b'_3 K_{\beta\beta 11} & 0 & 0 & 1 \\ -a'_4 + b''_4 K_{\beta\beta 11} & -a'_3 & -a'_2 & -a'_1 \end{bmatrix}$$

$$\mathbf{B}_V = \begin{bmatrix} 0 & 0 & 0 \\ 0 & 0 & 0 \\ b'_3 K_{\beta\alpha 11} & b'_3 K_{\beta\alpha 12} & b'_3 K_{\beta\beta 12} \\ b''_4 K_{\beta\alpha 11} & b''_4 K_{\beta\alpha 12} & b''_4 K_{\beta\beta 12} \end{bmatrix}$$

Appendix F. System data

F.1. Network parameters

- Base parameters: $S_{\mathrm{base}} = 100$ MVA; $\mathrm{fr}_{\mathrm{base}} = 50$ Hz; $U_{\mathrm{base}} = 660$ V.
- Network impedances (see Fig. 3): $Z_{\alpha\gamma} = 0.10 + 0.30\mathrm{j}$ p.u.; $Z_{\beta\gamma} = 0.03 + 0.15\mathrm{j}$ p.u.; $Z_\gamma = 1$ p.u.

F.2. Induction machine parameters

The wind park is formed by 86 fixed speed wind energy converters equipped with induction generators. The parameters for each induction machine are:

Nominal voltage: $V_{\alpha,\mathrm{nom}} = 660$ V
Nominal apparent power: $S_{\alpha,\mathrm{nom}} = 359$ kVA
Inertia constant: $H_\alpha = 3.025$ s
Stator resistance: $R_\alpha = 0.00571$ p.u.
Stator reactance: $X_s = 0.18781$ p.u.
Rotor resistance: $R_r = 0.00612$ p.u.
Rotor reactance: $X_r = 0.06390$ p.u.
Magnetizing reactance: $X_m = 2.78$ p.u.

and

$$T'_0 = \frac{X_r + X_m}{\omega_s R_r}$$

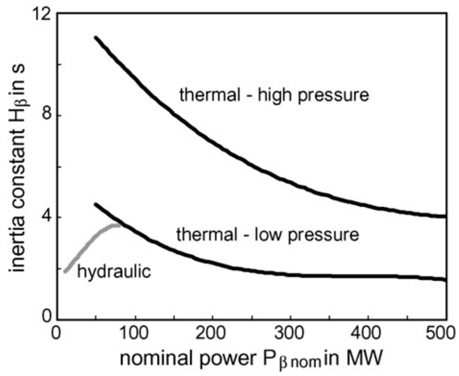

Fig. 15. Inertia constant H_β.

Table 1
Coefficients for the calculation of H_β

	Thermal		Hydraulic
	Low pressure	High pressure	
a_1	-7.2739×10^8	-3.2740×10^8	-4.6448×10^6
a_2	8.4003×10^5	6.3610×10^5	3.5120×10^4
a_3	-3.2605×10^2	-4.1484×10^2	2.8182×10^2
a_4	5.9833	12.971	1.5706

$$X_0 = X_s + X_m$$

$$X_\alpha = \frac{X_s + X_r X_m}{X_r + X_m}$$

The value for the shunt capacitor for the reactive compensation of induction machine is obtained from the following equality of reactances: $1/\omega_s C_\alpha = X_m$

F.3. Synchronous machine parameters

The transient reactance X_β is 0.3 p.u.

Values for the constant of inertia H_β in s (see Fig. 15) are obtained from Ref. [16]:

$$H_\beta = a_1 P^3_{\beta,\mathrm{nom}} + a_2 P^2_{\beta,\mathrm{nom}} + a_3 P^1_{\beta,\mathrm{nom}} + a_4 \qquad (52)$$

where $P_{\beta,\mathrm{nom}}$ is the nominal power in MW for the generation system and a_1, a_2, a_3 and a_4 are coefficients defined in Table 1.

F.4. Speed controller

$K_R = 10/(100\pi)$; $T_1 = 0.1$; $T_2 = 0.01$; $T_3 = 0.2$; $T_t = 0.3$

F.5. Voltage controller

$K_A = 120$; $K_F = 0.02$; $T_R = 0.01$; $T_A = 0.15$; $T_E = 0.5$; $T_F = 1$

$A_X = 0.01$; $B_X = 1.55$; $K_E = A_X B_X \mathrm{e}^{B_X E_{\beta 0}}$

References

[1] www.aeeolica.org.
[2] A. Larson, Flicker and slow voltage variations from wind turbines, in: Proceedings of the seventh ICHQP, Las Vegas, 1996.
[3] A. Larson, Flicker emission of wind turbines during continuous operation, IEEE Trans. Energy Convers. 17 (June (1)) (2001) 114–118.
[4] C. Carrillo, Analysis and simulation of isolated wind plants, Ph.D., Universidade de Vigo, Spain, 2001 (in Spanish).
[5] T. Thiringer, Periodic pulsations from a three-bladed wind turbine, IEEE Trans. Energy Convers. 16 (June (2)) (2001) 128–133.
[6] A.E. Feijóo, Influence of wind parks in steady-state security and power quality of electrical power systems, Ph.D., Universidade de Vigo, Spain, 1998 (in Spanish).
[7] C. Carrillo, A.E. Feijóo, J. Cidrás, J. González, Power fluctuations in an isolated wind plant, IEEE Trans. Energy Convers. 19 (1) (2004) 217–221.
[8] A.E. Feijóo, J. Cidrás, Analysis of mechanical power fluctuations in asynchronous WEC's, IEEE Trans. Energy Convers. 14 (September (3)) (1999) 284–291.
[9] D.S. Brereton, D.G. Lewis, C.C. Young, Representation of induction motor loads during power system stability studies, AIEE Trans. 76 (August) (1957) 451–461.
[10] P.C. Krause, Analysis of Electric Machinery, McGraw-Hill, 1986.
[11] J. Cidrás, A.E. Feijóo, A linear dynamic model for asynchronous wind turbines with mechanical fluctuations, IEEE Trans. Power Syst. 17 (3) (2002) 681–687.
[12] A.E. Feijóo, J. Cidrás, J.L.G. Dornelas, Wind speed simulation in wind farms for steady-state security assessment of electrical power systems, IEEE Trans. Energy Convers. 14 (February (4)) (2000) 1582–1588.
[13] R. Klose, F. Santjer, G. Gerdes, Flickerbewertung bei Windenergieanlagen, DEWI Magazin (August (11)) (1997) (in German).
[14] L.L. Freris, Wind Energy Conversion Systems, Prentice-Hall, 1990.
[15] J. Cidrás, A.E. Feijóo, C. Carrillo, Synchronization of asynchronous wind turbines, IEEE Trans. Power Syst. 17 (4) (2002) 1162–1169.
[16] P. Anderson, A.A. Fouad, Power System Control and Stability, IEEE Press, McGraw-Hill, 1993.
[17] G.J. Rogers, J.D. Manno, R.T.H. Alden, An aggregated motor model for industrial plants, IEEE Trans. Power Apparat. Syst. PAS-103 (April (4)) (1984).
[18] F. Nozari, M.D. Kankam, W.W. Price, Aggregation of induction motors for transient stability load modelling, IEEE Trans. Power Syst. PWRS-2 (November) (1987).
[19] P. Kundur, Power System Stability and Control, EPRI, McGraw-Hill, 1994.
[20] SIMULINK Dynamic System Simulation for MATLAB, The Mathworks Inc.
[21] Simpow Power System Simulation & Analysis Software, ABB Power System AB.
[22] Electromagnetic Compatibility (EMC)-Part 4: Testing and Measurement Techniques-Section 15: Flickermeter-Functional and Design Specifications, IEC 61 000-4-15, 1997.

C. Carrillo (1967) received his degree in electrical engineering from the Universidade de Vigo (Spain) in 1992 and his Ph.D. degree in electrical engineering in 2001. Since then he has been a lecturer in the Departamento de Enxeñería Eléctrica. His main fields of research are: harmonics, flicker and wind energy systems.

A.E. Feijóo (1965) received his degree in electrical engineering from the Universidade de Santiago de Compostela (Spain) and his Ph.D. degree in electrical engineering from the Universidade de Vigo (Spain). He is now a professor in the Departamento de Enxeñería Eléctrica of the Universidade de Vigo (Spain) and his current interest is wind energy and power quality.

J. Cidrás (1957) received his degree in electrical engineering from the Universidad de Las Palmas de G.C. (Spain). He obtained a Ph.D. in electrical engineering from the Universidade de Santiago (Spain) in 1987. He is a professor in the Departamento de Enxeñería Eléctrica of the Universidade de Vigo (Spain), and leads some investigation projects on wind energy, photovoltaic and planning of power systems. He is a member of IEEE.

J.F. Medina (1953) received his degree in electrical engineering from the Universidad de Las Palmas de G.C. (Spain) in 1983. He obtained a Ph.D. in electrical engineering from the Universidad de Las Palmas de G.C. in 1997. He is now a professor in the Departamento de Ingeniería Eléctrica and his current interest is wind energy and power quality.